**Atmospheric
Chemistry
and Physics
Discussions**

Laboratory investigation of photochemical oxidation of organic aerosol from wood fires – Part 2: Analysis of aerosol mass spectrometer data

A. P. Grieshop, N. M. Donahue, and A. L. Robinson

Center for Atmospheric Particle Studies, Carnegie Mellon University, Pittsburgh, PA, USA

Correspondence to: A. L. Robinson (alr@andrew.cmu.edu)

ACPD

8, 17095–17130, 2008

Laboratory studies of the atmospheric aging of wood smoke – Part 2

A. P. Grieshop et al.

Title Page

Abstract	Introduction
Conclusions	References
Tables	Figures

|◄ | ►|

◄ | ►

Back | Close

Full Screen / Esc

Printer-friendly Version

Interactive Discussion

Abstract

Experiments were conducted to investigate the effects of photo-oxidation on organic aerosol (OA) in dilute wood smoke by exposing emissions from soft- and hard-wood fires to UV light in a smog chamber. This paper focuses on changes in OA composition measured using a unit mass resolution quadrupole Aerosol Mass Spectrometer (AMS). The results highlight how photochemical processing can lead to considerable evolution of the mass, the volatility and the level of oxygenation of biomass-burning OA. Photochemical oxidation produced substantial new OA, more than doubling the primary contribution after a few hours of aging under typical summertime conditions. Aging decreased the OA volatility of the total OA as measured with a thermodenuder; it also made the OA progressively more oxygenated in every experiment. With explicit knowledge of the condensed-phase mass spectrum (*MS*) of the primary emissions from each fire, each *MS* can be decomposed into primary and residual spectra throughout the experiment. The residual spectra provide an estimate of the composition of the photochemically produced OA. These spectra are also very similar to those of the oxygenated OA that dominates ambient AMS datasets. In addition, aged wood smoke spectra are shown to be similar to those from OA created by photo-oxidized dilute diesel exhaust and aged biomass-burning OA measured in urban and remote locations. This demonstrates that the oxygenated OA observed in the atmosphere can be produced by photochemical aging of dilute emissions from combustion of fuels containing both modern and fossil carbon.

1   Introduction

Organic aerosols are a highly-dynamic system dominated by both variable gas-particle partitioning and chemical evolution. The sources of this organic material are not well understood, especially the relative contributions of primary versus secondary organic aerosol. Primary organic aerosols (POA) are directly emitted by a source in the con-

densed phase; secondary organic aerosols (SOA) are formed in the atmosphere via oxidation products of gas-phase precursors. Recent ambient measurements with the Aerodyne Aerosol Mass Spectrometer (AMS) have shown that oxygenated OA (OOA) is the dominant component of OA in most regions of the atmosphere (Zhang, 2007).

5 OOA is strongly correlated with secondary tracers such as inorganic species (Ulbrich et al., 2008; Zhang et al., 2005b) and odd oxygen (O_3+NO_2; or O_x) (Herndon et al., 2008) in ambient datasets. Therefore, OOA appears related to SOA; however, SOA generated in traditional smog chamber experiments (Bahreini et al., 2005) is spectrally distinct from ambient OOA. Additionally, laboratory SOA (Aiken et al., 2008) and

10 primary emissions (Mohr et al., 2008[1]) both have significantly lower O:C ratio than ambient OOA. In addition, field (de Gouw et al., 2008; de Gouw et al., 2005; Volkamer et al., 2006) and laboratory (Grieshop et al., 2008; Robinson, 2007; Sage et al., 2008; Weitkamp et al., 2007) measurements have shown that gas-phase oxidation can form much more SOA than is predicted by current models.

15 Recently, we have shown that photo-oxidation of diluted exhaust from a diesel engine produces substantial amounts of OA that is spectrally similar to OOA (Robinson, 2007; Sage et al., 2008). Although motor vehicles are an important source of aerosols in urban and regional environments, biomass burning is a much more important source at global scales. For example, biomass-burning is estimated to contribute 90% of the

20 global emissions of primary particulate organic carbon (OC) from combustion sources (Bond et al., 2004).

Aerosol emissions from biomass-burning are often identified using particle constituents such as chloride, potassium and levoglucosan (Simoneit et al., 1999). Recently, the contribution of biomass-burning emissions to urban OA concentrations has

---

[1]Mohr, C., Huffman, J. A., Cubison, M., Aiken, A. C., Docherty, K., Kimmel, J. R., Ulbrich, I. M., Hannigan, M., Garcia, J., and Jimenez, J. L.: Characterization of primary organic aerosol emissions from meat cooking, trash burning, and motor vehicles with high-resolution aerosol mass spectrometry and comparison with ambient and chamber observations, Environ. Sci. Technol., submitted, 2008.

Full Screen / Esc

Printer-friendly Version

Interactive Discussion

been estimated by factor analysis of ambient AMS data (DeCarlo et al., 2007; Lanz et al., 2007). However, source apportionment of biomass-burning emissions is complicated because these emissions evolve in the atmosphere. For example, dilution measurements show the gas-particle partitioning of these emissions depends on at-
5   mospheric conditions (Lipsky and Robinson, 2006; Shrivastava et al., 2006). Multiple field measurements report substantial in-plume production of OA (Abel et al., 2003; Lee et al., 2008; Nopmongcol et al., 2007; Reid et al., 1998, 2005). Other studies have observed substantial chemical evolution biomass-burning emissions with atmospheric aging but without additional production of OA (Capes et al., 2008; Hoffer et al., 2006).
10   This is the second paper in a two-part series that investigates the effects of photo-oxidation on wood smoke. As discussed in the companion paper (Grieshop et al., 2008), photo-oxidation of diluted wood smoke in a smog chamber produced substantial amounts of OA, essentially doubling OA concentrations after exposure to the equivalent of a few hours of summertime conditions. On average, less than 20% of this new
15   OA could be explained by oxidation of traditional SOA precursors. Results from a volatility basis-set model that explicitly tracks the partitioning and aging of low-volatility organics are compared to the chamber data and indicate that the OA production can be explained by oxidation of low-volatility organic vapors.

In this paper, we focus on the effects of photochemical aging on the composition of
20   organic aerosols emitted from biomass burning as measured with an AMS. The specific goals include:

1. quantify the production of secondary OA using a spectral decomposition method of Sage et al. (2008);

2. characterize the evolution of OA composition; and

25   3. compare results from these experiments to AMS data from the literature (laboratory and ambient) to place them in the broader context.

2 Experimental Methods

Exhaust from wood fires in a small wood stove was injected, via a heated inlet line, into a dark, temperature-controlled 12 m^3 Teflon-lined environmental chamber filled with HEPA and activated-carbon filtered air. Upon entering the chamber, the exhaust
5 rapidly mixed and cooled to 22±2°C. Initial particle concentrations were tens to hundreds of μg m^{-3} of predominantly carbonaceous material. The primary emissions were characterized for ~1 h and then the chamber UV lights were turned on to initiate photo-oxidation reactions. The evolution of the wood smoke was monitored using a suite of gas- and particle-phase instruments. Experimental details are discussed in a compan-
10 ion paper (Grieshop et al., 2008).

Separate experiments were conducted with mixed hardwoods, Laurel Oak and Yellow Pine, burning under a variety of conditions, from smoldering to active flaming combustion. Gas- and particle-phase concentrations inside the chamber were similar to field measurements of fresh biomass plumes (Grieshop et al., 2008). For example,
15 modified combustion efficiencies (MCE, Koppmann et al., 2005) ranged between 0.69 and 0.95 with a median value of 0.91. Organic to elemental carbon ratios of the fresh wood-smoke aerosol ranged from 1.1 to 13. Additional details on the experimental conditions are reported in a companion manuscript (Grieshop et al., 2008).

This paper focuses on data collected with a unit mass resolution quadrupole Aero-
20 dyne Aerosol Mass Spectrometer (Q-AMS) (Canagaratna et al., 2007). The AMS collected data with 5 min time resolution at a vaporizer temperature of 600°C, alternating between mass spectrum (*MS*) scanning, Jump Mass Spectrum (JMS, Crosier et al., 2007) and particle time of flight (PToF, (Jimenez et al., 2003) modes. The mass fragments scanned in PToF mode were selected to give information about the size distri-
25 butions and mixing states of the AMS species (organics, nitrate, potassium, etc.). The mass fragments scanned in JMS mode were selected to improve the signal-to-noise ratio for fragments of particular interest in organic mass spectra (e.g. *m/z* 44 and 57) and those expected to make significant contributions to wood burning POA (*m/z* 60,

73, 137 and 167 (Alfarra et al., 2007; Schneider et al., 2006). Except as noted below, the organic spectra were generated using the default fragmentation table (Allan et al., 2004).

We carefully considered the assignment of the AMS signal at m/z 28 and 18. Due to the difficulty of separating the organic particle signal (mostly from CO^+) from the large air beam signal (from N_2^+) at m/z 28, the default fragmentation table in the unit mass resolution AMS data analysis package has traditionally set the organic contribution at m/z 28 to zero (Allan et al., 2004). However, recent analysis of several ambient datasets suggests that the OA signal at m/z 28 in ambient samples is equivalent to the signal at m/z 44 (Aiken et al., 2008, and references therein). In these experiments, we directly estimated the contribution of OA to m/z 28 using particle-free samples to establish a baseline signal due to N_2^+. This correction is discussed in Sect. 3.2. Another complication is the uncertain contribution from organic dehydration fragments (H_2O^+) at m/z 18. In the original AMS fragmentation table (Allan et al., 2004), OA at m/z 18 set equal to the OA signal at m/z 44; Aiken et al. (2008) recently proposed reducing the OA contribution at m/z 18 to 0.225 times the OA signal at m/z 44. Here we have chosen to maintain the original fragmentation scheme for m/z 18. Since our biomass smoke was dominated by carbonaceous aerosol there should be minimal particle bound water under the low relative humidity conditions of these experiments (less than 20%). In addition, with the default fragmentation table, the AMS particle-bound water signal was always positive, which suggests that we have not over-apportioned m/z 18 to organics. Further, PToF data generally indicates that the particle signal at m/z 18 is aligned with, and of similar magnitude to, that at m/z 44. Updating the fragmentation scheme for m/z 18 to that proposed by Aiken et al. (2008) only has a minor effect on our results. For example, it reduces the AMS OA mass by 1 to 7% with corresponding increases in the relative contribution of other peaks.

2.1 Spectral decomposition of the AMS data

The AMS OA mass spectrum (MS) was decomposed into primary and secondary components using the residual spectrum approach (Sage et al., 2008). This approach uses the AMS signal at a single m/z as a tracer for primary OA. The residual spectrum ($MS_{residual}$) is defined as

$$MS_{residual}(t) = MS_{total}(t) - f_{tracer}(t) \times MS_{POA} \tag{1}$$

where $MS_{total}(t)$ is the measured OA MS at time t, MS_{POA} is the POA MS determined by averaging the AMS data for 15 to 25 min before turning on the chamber lights (i.e. before the initiation of photochemistry). The MS_{POA} is scaled using an estimate of the fraction of primary mass present (f_{tracer}),

$$f_{tracer}(t) = \frac{m_{tracer}(t)}{m_{tracer}(t_0)} \tag{2}$$

where $m_{tracer}(t)$ and $m_{tracer}(t_0)$ are the masses at the tracer peak at time t and at "lights-on", respectively.

The results from the spectral decomposition provide an estimate of the OA production in the chamber. We express this production as an OA enhancement ratio:

$$ER = \frac{m_{total}}{m_{POA}} = \frac{1}{f_{POA}} = \frac{1}{1 - f_{residual}} \tag{3}$$

where m_{total} and m_{POA} are the organic mass in the entire MS and attributed to the POA MS, and f_{POA} and $f_{residual}$ are the fractions of the total organic mass attributed to the POA and residual spectra, respectively.

The tracer peak is assumed to be a marker for the primary emissions. It can be selected based on a qualitative assessment of MS peak contributions (looking for peaks with individual contributions that do not respond to the initiation of photochemistry) and knowledge of likely primary markers. For example, previous experiments with diesel exhaust used m/z 57 (a marker for hydrocarbon-like organic aerosol – HOA) as the

17101

tracer peak (Sage et al., 2008). Here we used primary markers for wood smoke, including m/z 60, 73, 137 and 167 (Alfarra et al., 2007; Schneider et al., 2006). We also allowed the POA tracer peak to "float", by selecting the peak which minimizes the value of f_{tracer} for each individual MS; this is the first peak to go negative when sub-
5 tracting progressively larger amounts of the POA spectrum from the total spectrum. The algorithm minimizes f_{tracer} under the constraints that:

   a) in the total MS, a fragment has a signal-to-noise ratio greater than three and contributes at least 0.5% of the total mass, and

   b) in the POA MS that the peak varies by less than 10% among the AMS scans that
10   are averaged to yield the POA spectrum.

Our previous work with diesel exhaust demonstrated that the primary-secondary split determined by the spectral decomposition method agrees well with estimates based on other methods (Sage et al., 2008; Weitkamp et al., 2007). However, the residual approach assumes that the POA spectrum is constant in time and that the tracer peak is
15 a conserved tracer for the POA. This means that POA composition does not evolve due to heterogeneous processing or changes in gas-particle partitioning. If the compound associated with the tracer peak is heterogeneously oxidized or evaporates during an experiment then the spectral decomposition method based on this peak will underestimate the contribution of POA. Alternatively, if the tracer peak is produced by secondary
20 chemistry then the spectral decomposition method will overestimate the contribution of POA. These assumptions and associated issues are discussed in more detail by Sage et al. (2008).

2.2 OA Volatility

Particle volatility was measured with a thermodenuder (TD) system that first heated the
25 aerosol and then stripped the evaporated gas-phase components using an activated-carbon denuder (An et al., 2007). Gas temperatures in the heated zone ranged between 50 and 85°C; the residence time in the heated section was approximately 16 s.

Measurements were taken with an SMPS and the AMS downstream from the *TD* system and a bypass line maintained at 25°C. The instruments were switched between these two lines every 15 to 30 min.

OA evaporation in the *TD* is quantified using the mass fraction remaining (MFR):

$$\text{MFR} = \frac{C_{TD}}{C_{\text{bypass}}} \tag{4}$$

where C_{TD} and C_{bypass} are the AMS concentrations measured downstream of the *TD* and bypass lines, respectively. MFRs were calculated for the bulk OA and individual AMS mass fragments. Total number loss in the *TD* system was found to be less than 2% (An et al., 2007) and loss of non-refractory mass measured by the AMS less than 5% at ambient temperatures. Previously published data with similar *TD* designs (Huffman et al., 2008; Wehner et al., 2002) suggest that mass loss in our particle size- and *TD* temperature-ranges would be on the order of 5 to 10%. No adjustments were made for these losses.

3   Results

3.1   OA production estimates via spectral decomposition

Photo-oxidation of the diluted wood smoke inside the chamber created substantial new OA mass (Grieshop et al., 2008). Figure 1 compares estimates of OA production derived using the spectral decomposition method to results based on using black carbon (BC) as the tracer for chamber wall loss. The BC-based approach is discussed in the companion manuscript (Grieshop et al., 2008). The results are presented in terms of an OA enhancement ratio (ER), which quantifies OA production relative to the initial POA concentration. For example, an OA enhancement ratio of two indicates that photo-oxidation has doubled the wall-loss corrected OA concentration in the chamber.

Figure 1 plots OA enhancement ratios calculated using different mass fragments associated with primary wood smoke OA (m/z 60, 73, 137 and 167) (Alfarra et al., 2007; Schneider et al., 2006) and the floating-peak residual method described in Sect. 2.1.

The floating-peak method predicts that photo-oxidation doubles or triples the OA
5 mass after about five hours under typical summertime conditions. These estimates are comparable to those derived using the BC method. However, the tracer fragment identified by the floating-peak method for the primary OA varied from experiment to experiment. In the two experiments shown in Fig. 1, the floating-peak method identified m/z 137 and 167 as the tracer fragment for primary emissions in one experiment
10 (Fig. 1a) and m/z 60 in a second (Fig. 1b). In other experiments (not shown) m/z 113, 165 and 152 were identified as tracers for primary OA. In contrast, application of the residual method to diesel exhaust always identifies m/z 57 as the primary tracer fragment (Sage et al., 2008). This highlights the inherent variability in wood-smoke POA and underscores the challenges associating with using a single spectral marker
15 for biomass-burning OA.

In every experiment at least one of the AMS mass fragments identified as a marker for primary OA from wood smoke yields a poor estimate for the OA production. For example, using either m/z 60 or 73 as the tracer fragment for the residual decomposition greatly underestimates the OA production in the experiment shown in Fig. 1a. In
20 this experiment (and two others, see Fig. 5b for m/z 60 data) the relative contribution of these mass fragments was very low and did not change with aging. This suggests some secondary production of these mass fragments; for example, smog-chamber experiments with traditional SOA precursors produce modest amounts of organic mass at m/z 60 (between 0.3 and 0.6% of the total signal) (Bahreini et al., 2005; Ulbrich and
25 Jimenez, 2008) while ambient OOA spectra in the absence of strong biomass-burning influence have ∼0.2–0.3% of the signal at m/z 60 (Ulbrich et al., 2008; Zhang et al., 2005a). In the experiment shown in Fig. 1b, the ER estimated using m/z 137 as the POA tracer is substantially higher than other estimates. This means that the relative contribution at m/z 137 decays more quickly than the other peaks, potentially due to

heterogeneous oxidation and/or preferential evaporation. The *TD* data discussed below support the aging hypothesis because m/z 137 is found to be one of the least volatile peaks in the spectrum.

⁵ The particle size distributions measured by the AMS provide another indication of the substantial production of new OA during photo-oxidation. Figure 2 shows size distributions for selected AMS fragments associated with primary (m/z 60 and m/z 39) and secondary material (m/z 44 and m/z 46). The fragment at m/z 44 is a marker for oxygenated organics (Zhang et al., 2005a; Zhang et al., 2005b), while m/z 60 is a marker for primary wood-smoke OA (Alfarra et al., 2007; Schneider et al., 2006). K^+

¹⁰ and organics contribute to the AMS signal at m/z 39. NO_3^+ and organics contribute to the AMS signal at m/z 46. Figure 2a shows that in our fresh wood-smoke samples all of these fragments have a modal vacuum aerodynamic diameter (d_{va}) of about 180 nm. Figure 2b indicates that aging increased the mode of the particle size distribution to about 250 nm and increased the relative contribution of secondary fragments (m/z

¹⁵ 44 and 46); clear evidence of particle growth driven by condensation of secondary species. All of the mass fragments have essentially the same size distribution, which suggests that the particles are internally mixed.

3.2 Evolution of OA chemical composition

The AMS data provide insight into the evolution of the chemical nature of the OA.
²⁰ Figure 3a compares a portion of the organic *MS* of emissions from a smoldering Yellow Pine fire measured at the beginning and the end of an experiment. The spectrum of the fresh POA is qualitatively similar to published wood-burning spectra (Alfarra et al., 2007; Schneider et al., 2006) with dominant peaks at 15, 18, 27, 29, 41 and 43. After 5 h of aging, the relative contributions from peaks associated with oxygenated OA, such
²⁵ as m/z 29 (CHO^+), 43 ($C_2H_3O^+$, also $C_3H_7^+$) and 44 (CO_2^+) have grown significantly. The aged spectra also show a substantial increase in the particle signal at m/z 46, evidence of the production of nitrate (presumably organic in nature due to the lack of ammonium in the chamber) during the photo-oxidation.

A noteworthy difference between the spectra shown in Fig. 3a and previously published AMS results is that m/z 28 is frequently the largest contributor to the organic mass spectrum. This was observed in every experiment. Evidence for the substantial OA signal at m/z 28 is shown in Fig. 4. Figure 4a shows size distributions of se-
lected m/z measured in PToF mode. The signal at m/z 28 is large at small diameters due to gas-phase N_2^+ but there is also an unequivocal particle-phase signal peaking at approximately 150 nm aligned with the other m/z from wood-smoke POA, including 44, 60, 73 and 137. Figure 4b shows a time series of the raw ion signal at m/z 28. The dashed line and lower hatched area indicate the baseline signal from gas-phase
N_2^+ derived from measurements made before wood smoke was injected in the chamber and measurements made at the end of the experiment through a HEPA filter. The dashed line is a linear interpolation between these measurements. The baseline m/z 28 signal shows the expected decay due to degradation of the AMS electron multiplier during the experiment (Allan et al., 2003). Figure 4b shows that there was a substantial
increase in the m/z 28 signal above this baseline when wood smoke was injected into the chamber.

We estimated the particle-phase contribution at m/z 28 as the signal above a baseline air-beam signal shown in Fig. 4b. This estimate was in good general agreement with similar estimates derived from the integration of PToF gas- and particle-phase
data (see Zhang et al., 2005a) for description of method). The approximate uncertainty in the estimated m/z 28 particle signal is ±25% based on intercomparison of the estimates from these two methods. Figure 4c plots the time series of the ratio of the organic-equivalent masses at m/z 28 to 44. In this experiment, m/z 28 initially contributes 8 times more OA than m/z 44. Across the entire set of experiments, m/z 28
contributed 10 to 25% of the OA in fresh wood smoke POA – a factor of 4 to 10 higher than the organic contribution at m/z 44. Figure 4c indicates that this ratio decreases rapidly to about two after about half an hour of photochemical aging. Several studies have shown that the organic signal at m/z 28 can be comparable or larger than that at m/z 44 for ambient organics (Aiken et al., 2008; Takegawa et al., 2007; Zhang et al.,

Printer-friendly Version

Interactive Discussion

2005a). Aiken et al. (2008) have proposed that the organic fragmentation table used in the AMS software for ambient studies be updated to set the organic contribution at m/z 28 (mostly CO^+) equal to that at m/z 44. Our results suggest that this may be too small for fresh wood smoke samples. Although m/z 28 appears to be an important
5 contributor to the OA *MS* in these experiments, we neglect its contribution in plots of fragment contributions (Figs. 3b, 5 and 7) in order to facilitate direct comparisons of our data with published AMS data that are based on the Allan et al. (2004) fragmentation table.

Figure 3b shows a time series of the fractional contribution of selected AMS mass
10 fragments to the total organic spectrum from a typical experiment. First we discuss fragments associated with primary emissions. Fragments at m/z 60, 73, 137 and 167 are associated with biomass burning emissions (Alfarra et al., 2007; Schneider et al., 2006) and the unit mass-resolution AMS fragment at 57 ($C_4H_9^+$, but also $C_3H_5O^+$) is commonly associated with reduced organics emitted from fossil-fuel combustion
15 sources (Zhang, 2007). After the lights were turned on, the relative contribution of all of these POA-associated peaks decreased, especially during the first 2 h of aging. This decrease is due to the production of substantial new OA mass. Some of the primary fragments (m/z 57, 60 and 73) also decreased before the UV lights were turned on. We attribute this decrease to evolving gas-particle partitioning associated with the
20 initial dilution of the exhaust that occurred when the exhaust was first injected into the chamber. In-chamber dilution experiments have shown that equilibration after dilution can occur on time scales on the order of hours (Grieshop et al., 2007, 2008[2]). As discussed below, the *TD* measurements indicate that m/z 57, 60 and 73 are some of the most volatile fragments in the AMS spectra.
25 Figure 3b also plots time series of AMS mass fragments associated with OOA components, such as m/z 44 and 43. The fractional contributions at m/z 44 and 43 to total OA mass have been used as an indicator of OOA and OOA-II, respectively, in ambient

---

[2]Grieshop, A. P. and Robinson, A. L.: Gas-particle partitioning of fresh diesel emissions at near-ambient concentrations, in preparation, 2008.

data sets (Ulbrich et al., 2008; Zhang et al., 2005a; Zhang, 2007). The relative contribution of m/z 44 (CO_2^+) increased throughout the aging phase of every experiment, mirroring the production of OA. This means that OA formed during photo-oxidation was more oxygenated than the fresh, primary OA. In this experiment, the fractional contribution at m/z 43 increased from 4 to 6% of the OA mass within the first 2 h of aging after which it remained constant. m/z 43 is associated with both hydrocarbon/primary ($C_3H_7^+$) and secondary/oxygenated ($C_2H_3O^+$) components of the aerosol. The relative contribution at m/z 28 also increased with aging, but less than that at m/z 44. As a result, the approximate ratio of m/z 28 and 44 was reduced from 4 to 2 during aging.

High molecular weight mass fragments contribute a substantial fraction of the wood smoke POA. Figure 3b shows that approximately 25% of the initial OA mass is found at mass fragments with m/z larger than 100; after 5.5 h of aging the contribution of these fragments drops to 11%. Therefore, the OA produced in the chamber is composed of smaller molecules and/or species less resistant to fragmentation in the AMS. High mass fragments contribute an even smaller fraction (∼3%) of ambient OOA spectra (Zhang et al., 2005a).

Figure 5 plots the time series for the fractional contribution for two important mass fragments, m/z 44 and 60, measured in all of the experiments (the values neglect the contribution at m/z 28 to the OA mass to facilitate comparison with published AMS data). These experiments spanned a range of burning conditions and fuel types (Grieshop et al., 2008). Figure 5a shows that the contribution from m/z 44 increased during photo-oxidation in every experiment. For the Oak experiments, the initial contribution at m/z 44 ranged from 4 to 8% (3.5 to 5.5% if the contribution m/z 28 is included in the OA mass) and was enhanced by a factor of 1.6 to 2 with aging. Pine experiments had initial m/z 44 contributions of 1.5 to 3.9% (1.2 to 3% if the particle contribution at m/z 28 is accounted for) which were enhanced by a factor of 2.2 to 5.6 with aging. Therefore, in every experiment, photo-oxidation created more oxygenated OA.

Figure 5b indicates that the fractional contribution at m/z 60 exhibited more variation

across the set of experiments. In some experiments there was a significant contribution to the POA from m/z 60: 1 to 4% of the organic mass, comparable to the 0.5 to 4% range reported for fresh biomass burning emissions (Schneider et al., 2006). However, in other experiments, m/z 60 contributed minimally to the POA (less than 0.5%), and the fractional contribution at this fragment remained basically constant throughout the entire experiment, consistent with some secondary production. If m/z 60 is used as the tracer for the primary emissions in these experiments the residual decomposition method predicts very little OA production (e.g. Fig. 1a).

Figure 6 plots measurements of OA evaporation as a function of thermodenuder temperature. Results are shown for both the total AMS organic signal and selected AMS mass fragments for both fresh emissions and those aged for 4 h. The results are averages across all of the experiments. The volatility of the bulk OA is discussed in detail in the companion paper (Grieshop et al., 2008). Figure 6 indicates that, on average, about 60% of the fresh POA evaporated at 50°C and that aging decreased the volatility of the OA.

Fragments associated with POA show a range of volatilities: m/z 60, 73 and 57 are among the most volatile fragments while m/z 137 is one of the least volatile fragments. After aging, higher temperatures were required to evaporate the same amount of these primary fragments in the wood smoke. The relative volatility of the different fragments in the aged aerosol (Fig. 6b) is similar to that in fresh OA (Fig. 6a), but shifted to roughly align with the behavior of the bulk OA. Therefore, even after aging, fragments at m/z 60, 73 and 57 are substantially more volatile than the bulk OA. The cause for this apparent shift in volatility of the primary fragments with aging is not known. This shift could indicate an actual change in volatility or may be due to differences in the evaporation rates of fresh and aged aerosol inside the thermodenuder. Although Fig. 6 is based on average data, the trends discussed were observed in every experiment.

Figure 6 shows that the fragment at m/z 44 is always less volatile than the bulk aerosol, indicating that the more oxidized components of OA have lower volatilities. For example, partial evaporation in the *TD* increases the fractional contribution of m/z

44. This is illustrated in Fig. 7, which presents time series of the fractional contribution at m/z 44 and thermodenuder data measured during an experiment conducted with emissions from smoldering Yellow Pine. This has been previously shown in both laboratory and field studies (Grieshop et al., 2007; Huffman et al., 2008[3]).

Figure 7 indicates that the fractional contribution of m/z 44 is not a perfect measure of the overall OA volatility in these experiments. For example, aging caused the fractional contribution of m/z 44 to monotonically increase throughout every experiment, but the OA MFR measured at 50°C shows a step change in volatility (see also Fig. 5 in the companion manuscript of Grieshop et al., 2008). This implies that volatility of the SOA evolved over the course of the experiment. Specifically it suggests that the SOA initially created by aging is somewhat less volatile and less oxygenated than that formed later in the experiment. This can occur because volatility depends on both molecular weight and extent of oxygenation. For example, the initial burst of SOA formation could be associated with oxidation of relatively reduced semivolatile vapors that create very low-volatility but not very oxygenated products. Later in the experiment second- and third-generation precursors may become more important. These later-generation precursors may have lower molecular weights than the first-generation precursors due either to fragmentation or multigenerational processing of initially more volatile precursors. In this situation, the SOA formed from later-generation precursors could be highly-oxygenated, but not necessarily less volatile than the first generation SOA.

3.3 Intercomparison of AMS spectra

Figure 8 compares three AMS organic spectra. Two of the spectra are from a pine-fire aging experiment; Fig. 8a is an average of the fresh (un-aged) wood-smoke POA

---

[3] Huffman, J. A., Aiken, A. C., Docherty, K. S., Ulbrich, I. M., DeCarlo, P. F., Jayne, J. T., Onasch, T. B., Trimborn, A., Worsnop, D. R., Ziemann, P. J., and Jimenez, J. L.: Volatility of primary and secondary organic aerosols in the field contradicts current model representations, Environ. Sci. Technol., submitted, 2008.

measured before the chamber lights were turned on and Fig. 8c plots the residual spectrum from this experiment after four hours of aging derived using m/z 60 as the POA tracer. This residual spectrum is the approximate AMS signature of the OA that was photochemically produced during the experiment (Sage et al., 2008). Figure 8e shows the OOA spectrum derived from the ambient data collected during the Pittsburgh Air Quality Study (Ulbrich and Jimenez, 2008; Zhang et al., 2005a). Figure 8b and d shows difference spectra.

The difference spectrum plotted in Fig. 8b indicates that the fresh wood-smoke POA is quite distinct from the aged residual; for example, fresh wood-smoke POA has a much larger contribution at higher-mass peaks than the residual spectrum. Oxygenated peaks such as m/z 44 are also much more significant in the residual than the POA spectrum. In comparison, the difference spectrum shown in Fig. 8d indicates that this residual spectrum is quite similar to Pittsburgh OOA.

Linear regression of relative spectral intensities can be used to quantitatively compare AMS data (Alfarra et al., 2006; Schneider et al., 2006). The approach is illustrated by the scatter plots shown as insets in Fig. 8a and e. For this analysis, the spectral contributions at m/z 16, 17 and 18 have been excluded in the correlations because they all depend via uncertain fragmentation schemes on m/z 44. The contribution at m/z 28 has also been excluded because it has traditionally been neglected in the AMS fragmentation scheme. Linear regression of the fresh wood-smoke spectrum versus the residual spectrum plotted as an inset in Fig. 8a yields slope, intercept and R^2 values of 0.42, 0.19 and 0.64, respectively. This underscores that wood-smoke POA and OA produced by photo oxidization have distinct spectral signatures in the AMS. As expected from the difference spectra shown in Fig. 8d, a very strong correlation is observed between the residual spectra and Pittsburgh OOA (slope=1.01, intercept=0.00, R^2=0.93); therefore photo-oxidation of biomass smoke generates OOA similar to that observed in the atmosphere.

To illustrate how the wood-smoke OA evolves with aging, Fig. 9 compares AMS data from one experiment to eight different reference spectra. Each trace plotted in Fig. 9

indicates the R^2, slope or intercept of a linear regression of our total OA spectra versus one of the reference spectra. Since we measured an AMS spectrum every 5 min, the results are presented as a time series to show the evolving linear correlation of our data versus one of the reference spectra. As previously discussed, the contributions at

5 m/z 16, 17, 18 and 28 are also excluded from this analysis.

Figure 9a compares our spectra to ambient AMS data thought to be strongly influenced by biomass burning. We consider two biomass-burning OA (BBOA) factors derived from ambient measurements made in Mexico City during the MILAGRO campaign (Aiken et al., 2008; DeCarlo et al., 2007). One of the Mexico City BBOA factors

10 is based on ground measurements made during the early morning and is therefore thought to be dominated by relatively fresh primary emissions (Aiken et al., 2008). The other Mexico City BBOA factor is based on measurements made aloft from a C-130 aircraft during the late morning and afternoon (DeCarlo et al., 2007); this BBOA factor is thus likely aged in a similar way to what is observed in our study. We also consider

15 a total OA spectra measured in a biomass-burning plume from Siberian forest fires at 5.5 km of altitude over Alaska from the NASA DC-8 aircraft during the ARCTAS-1 field campaign (all spectra from Jimenez, personal communication, 2008). The ARCTAS data is expected to be even more aged than either of the MILAGRO factors.

Of all of the reference spectra considered here, Fig. 9 indicates that our fresh primary OA data are most correlated with Mexico City BBOA factor derived from the early morning ground-based measurements (R^2=0.78; slope=0.90; intercept=0.15).

20 Biomass burning is a highly variable source and this level of correlation is comparable to that observed amongst different fresh wood-smoke spectra measured during source tests. For example, R^2 values among our POA spectra collected during different experiments ranged between 0.5 to 0.95, which is comparable to correlations of our POA

25 spectra with other published biomass burning data (Bahreini et al., 2005; Schneider et al., 2006; Ulbrich and Jimenez, 2008). Aging causes our data to become progressively less correlated with the MILAGRO ground-based BBOA factor. This supports the conclusion that the early morning ground measurements made during MILAGRO were

Laboratory studies of the atmospheric aging of wood smoke – Part 2

A. P. Grieshop et al.

strongly influenced by fresh biomass burning emissions.

Our fresh POA emissions are not well correlated with the two aged BBOA spectra measured aloft. However, photo-oxidation causes our measured spectra to become progressively more correlated to the two aged BBOA factors (MILAGRO airborne and ARCTAS-1). After five hours of aging there is excellent agreement with both of these factors; for example a linear regression with the MILAGRO aloft factor yields an R^2=0.90, slope=0.97 and intercept=0.03. A similar trend is seen with spectra from our other experiments, with the aged BBOA factors showing a stronger correlation to spectra collected after more aging. This highlights the dynamic character of the chemical composition of biomass-burning emissions and that the photochemical age of air masses should be considered when interpreting results from factor analysis of ambient data sets.

Figure 9b compares our wood-smoke spectra to HOA and OOA factors derived from the Pittsburgh Air Quality Study dataset (Ulbrich and Jimenez, 2008; Zhang et al., 2005a). As expected, wood-smoke spectra (fresh or aged) are not similar to HOA factor, which is associated with fresh emissions from internal combustion sources such as vehicles. Our fresh wood-smoke spectra are also not that similar to the ambient OOA factor. This indicates that OOA and primary BBOA can be distinguished by factor-analysis techniques. However, aging causes the wood-smoke spectrum to become increasingly correlated with the reference OOA spectrum. After about one hour of aging, the aged wood-smoke spectra has become well-correlated with Pittsburgh OOA spectrum (R^2=0.89, slope=0.45, intercept=0.12). The small slope suggests that our total wood-smoke OA is less oxidized than the Pittsburgh OOA. This is not surprising since our total spectrum contains significant primary and secondary components. As shown in the inset panel in Fig. 8e, much better agreement is observed if one compares our residual spectrum (not total OA spectrum) with the Pittsburgh OOA. The residual spectrum is our best estimate of the spectral signature of the OA produced during the experiments.

Figure 9c compares our wood-smoke data to reference spectra measured dur-

A. P. Grieshop et al.

ing similar experiments conducted with diesel-engine emissions (Sage et al., 2008; Weitkamp et al., 2007). We consider three reference spectra from the diesel experiments: fresh primary emissions (diesel POA); the total OA spectrum after 5 h of aging; and the residual spectra after 5 h of photo-oxidation. As expected, there is little correlation between the fresh diesel POA and any of the AMS data from the wood smoke experiments. Therefore we conclude that fresh primary diesel emissions and wood smoke have distinct AMS signatures, consistent with previous studies. However, aging of wood smoke creates OA that becomes progressively more similar to the aged diesel emissions. For example, after two hours of aging, the wood-smoke OA spectra are strongly correlated with both the aged diesel total OA reference spectrum (R^2=0.89, slope=0.89, intercept=0.04) and the aged diesel residual reference spectrum (R^2=0.88, slope=0.61, intercept=0.12). Therefore, photo-oxidizing diluted emissions from these very different sources creates OA with similar chemical profiles as measured by a Q-AMS. This occurs even though fresh diesel and wood-smoke emissions are chemically distinct – diesel emissions are dominated by saturated species (e.g. straight-chain and cyclic alkanes and aromatic species) (Schauer et al., 1999) while wood smoke is composed of more oxygenated species (e.g. sugars, resin acids and phenols) (Schauer et al., 2001). This underscores the significant role of atmospheric processing in altering and homogenizing the composition of atmospheric OA.

Although Figs. 8 and 9 present data from a single experiment, similar trends are observed in every experiment. In addition, the conclusions hold even if one considers only a subset of the AMS data, for example m/z larger than 44 (an approach used to mitigate the influence in the R^2 calculation of the high contributions from smaller masses in AMS spectra).

4   Discussion and conclusions

This paper and its companion (Grieshop et al., 2008) demonstrate that photo-oxidation of diluted wood-combustion emissions in a smog chamber rapidly produces substantial

OA with a chemical character quite distinct from the primary emissions. After several hours of aging under atmospherically relevant conditions, the unit mass resolution AMS spectrum of this new OA is very similar to the spectrum of OOA that dominates ambient OA levels in many locations (DeCarlo et al., 2007; Zhang et al., 2005a).

5   We have now demonstrated that photo-oxidation of emissions from combustion of fossil fuels (Robinson, 2007; Sage et al., 2008) and modern fuels (this work) produce substantial amounts of OA with a unit-resolution AMS spectrum closely resembling OOA. In contrast, traditional SOA sources – oxidation of VOC precursors – have not; for example, mass spectra from monoterpene plus ozone reactions are markedly differ-

10 ent from OOA (Alfarra et al., 2006; Bahreini et al., 2005; Zhang et al., 2006). However, traditional SOA experiments typically only consider first- or early-generation oxidation products. These products constitute a pool of semivolatile compounds similar in volatility to the fresh diesel and fresh biomass burning sources we are discussing here. It is possible that this 'fresh traditional' SOA can also be aged to yield something more

15 closely resembling OOA. This aging appears to dominate ambient OA outside of urban centers, no matter what the original OA source – primary emissions, oxidation of volatile precursors, fossil or modern. Given that atmospheric oxidation chemistry is not overly selective, it is also quite possible that the relatively uniform character of OOA is due to photo-oxidation of emissions from different sources producing chemically similar

20 material and not simply an artifact of the fragmentation that occurs inside the AMS.

    The results of this study lend support to the use of factor analysis to help interpret ambient AMS data. For example, the spectral characteristics of fresh and aged BBOA are distinct from fresh motor-vehicle emissions. Our study further reinforces the connection between OOA and OA formed from photo-chemistry. In fact, with unit-

25 mass-resolution AMS data alone, it is difficult to distinguish OOA (derived from factor analysis of ambient data) from OA formed from the laboratory aging of biomass burning emissions or diesel emissions. In addition, the substantial evolution of wood smoke (and diesel) spectra with aging underscores the challenges associated with trying to use static factors to represent emissions of different sources.

References

Abel, S. J., Haywood, J. M., Highwood, E. J., Li, J., and Buseck, P. R.: Evolution of biomass burning aerosol properties from an agricultural fire in Southern Africa, Geophys. Res. Lett., 30(15), 1783, doi:10.1029/2003GL017342, 2003.

Aiken, A. C., DeCarlo, P. F., Kroll, J. H., Worsnop, D. R., Huffman, J. A., Docherty, K. S., Ulbrich, I. M., Mohr, C., Kimmel, J. R., Sueper, D., Sun, Y., Zhang, Q., Trimborn, A., Northway, M., Ziemann, P. J., Canagaratna, M. R., Onasch, T. B., Alfarra, M. R., Prevot, A. S. H., Dommen, J., Duplissy, J., Metzger, A., Baltensperger, U., and Jimenez, J. L.: O/C and OM/OC ratios of primary, secondary, and ambient organic aerosols with high-resolution time-of-flight aerosol mass spectrometry, Environ. Sci. Technol., 2(12), 4478–4485, 2008.

Alfarra, M. R., Paulsen, D., Gysel, M., Garforth, A. A., Dommen, J., Prévôt, A. S. H., Worsnop, D. R., Baltensperger, U., and Coe, H.: A mass spectrometric study of secondary organic aerosols formed from the photooxidation of anthropogenic and biogenic precursors in a reaction chamber, Atmos. Chem. Phys., 6, 5279–5293, 2006,
http://www.atmos-chem-phys.net/6/5279/2006/.

Alfarra, M. R., Prévôt, A. S. H., Szidatt, S., Sandradewi, J., Weimer, S., Lanz, V. A., Schreiber, D., Mohr, M., and Baltensperger, U.: Identification of the mass spectral signature of organic aerosols from wood burning emissions, Environ. Sci. Technol., 41(16), 5770–5777, 2007.

Allan, J. D., Delia, A. E., Coe, H., Bower, K. N., Alfarra, M. R., Jimenez, J. L., Middlebrook, A. M., Drewnick, F., Onasch, T. B., Canagaratna, M. R., Jayne, J. T., and Worsnop, D. R.: A generalised method for the extraction of chemically resolved mass spectra from aerodyne aerosol mass spectrometer data, J. Aerosol Sci., 35(7), 909–922, 2004.

Allan, J. D., Jimenez, J. L., Williams, P. I., Alfarra, M. R., Bower, K. N., Jayne, J. T., Coe, H., and Worsnop, D. R.: Quantitative sampling using an Aerodyne aerosol mass spectrometer:

Laboratory studies of the atmospheric aging of wood smoke – Part 2

A. P. Grieshop et al.

Title Page	
Abstract	Introduction
Conclusions	References
Tables	Figures

◄◄	►►
◄	►
Back	Close

Full Screen / Esc

Printer-friendly Version

Interactive Discussion

1. Techniques of data interpretation and error analysis, J. Geophys. Res.-Atmos., 108(D3), 4090, doi:10.1029/2002JD002358, 2003.

An, W. J., Pathak, R. K., Lee, B., and Pandis, S. N.: Aerosol volatility measurement using an improved thermodenuder: Application to secondary organic aerosol, J. Aerosol Sci., 38(3), 305–314, 2007.

Bahreini, R., Keywood, M. D., Ng, N. L., Varutbangkul, V., Gao, S., Flagan, R. C., Seinfeld, J. H., Worsnop, D. R., and Jimenez, J. L.: Measurements of secondary organic aerosol from oxidation of cycloalkenes, terpenes, and m-xylene using an Aerodyne aerosol mass spectrometer, Environ. Sci. Technol., 39(15), 5674–5688, 2005.

Bond, T. C., Streets, D. G., Yarber, K. F., Nelson, S. M., Woo, J. H., and Klimont, Z.: A technology-based global inventory of black and organic carbon emissions from combustion, J. Geophys. Res.-Atmos., 109(D14), D14203, doi:10.1029/2003JD003697, 2004.

Canagaratna, M. R., Jayne, J. T., Jimenez, J. L., Allan, J. D., Alfarra, M. R., Zhang, Q., Onasch, T. B., Drewnick, F., Coe, H., Middlebrook, A., Delia, A., Williams, L. R., Trimborn, A. M., Northway, M. J., DeCarlo, P. F., Kolb, C. E., Davidovits, P., and Worsnop, D. R.: Chemical and microphysical characterization of ambient aerosols with the aerodyne aerosol mass spectrometer, Mass Spectrom. Rev., 26(2), 185–222, 2007.

Capes, G., Johnson, B., McFiggans, G., Williams, P. I., Haywood, J., and Coe, H.: Aging of biomass burning aerosols over West Africa: aircraft measurements of chemical composition, microphysical properties and emission ratios, J. Geophys. Res., in press, 2008.

Crosier, J., Jimenez, J. L., Allan, J. D., Bower, K. N., Williams, P. I., Alfarra, M. R., Canagaratna, M. R., Jayne, J. T., Worsnop, D. R., and Coe, H.: Technical Note: Description and use of the new Jump Mass Spectrum mode of operation for the Aerodyne Quadrupole Aerosol Mass Spectrometers (Q-AMS), Aerosol Sci. Tech., 41(9), 865–872, 2007.

de Gouw, J., Brock, C., Atlas, E., Bates, T., Fehsenfeld, F., Goldan, P., Holloway, J., Kuster, W., Lerner, B., and Matthew, B.: Sources of particulate matter in the northeastern United States in summer: 1. Direct emissions and secondary formation of organic matter in urban plumes, J. Geophys. Res, 113, D08301, doi:10.1029/2007JD009243, 2008.

de Gouw, J. A., Middlebrook, A. M., Warneke, C., Goldan, P. D., Kuster, W. C., Roberts, J. M., Fehsenfeld, F. C., Worsnop, D. R., Canagaratna, M. R., Pszenny, A. A. P., Keene, W. C., Marchewka, M., Bertman, S. B., and Bates, T. S.: Budget of organic carbon in a polluted atmosphere: results from the New England Air Quality Study in 2002, J. Geophys. Res.-Atmos., 110(D16), D16305, doi:10.1029/2004JD005623, 2005.

Laboratory studies of the atmospheric aging of wood smoke – Part 2

A. P. Grieshop et al.

Title Page

Abstract	Introduction
Conclusions	References
Tables	Figures

|◄ | ►|

◄ | ►

Back | Close

Full Screen / Esc

DeCarlo, P. F., Dunlea, E. J., Kimmel, J. R., Aiken, A. C., Sueper, D., Crounse, J., Wennberg, P. O., Emmons, L., Shinozuka, Y., Clarke, A., Zhou, J., Tomlinson, J., Collins, D. R., Knapp, D., Weinheimer, A. J., Montzka, D. D., Campos, T., and Jimenez, J. L.: Fast airborne aerosol size and chemistry measurements above Mexico City and Central Mexico during the MILAGRO campaign, Atmos. Chem. Phys., 8, 4027–4048, 2008, http://www.atmos-chem-phys.net/8/4027/2008/.

Grieshop, A. P., Donahue, N. M., and Robinson, A. L.: Is the Gas-Particle Partitioning in alpha-Pinene Secondary Organic Aerosol Reversible?, Geophys. Res. Lett., 34, L14810, doi:10.1029/2007GL029987, 2007.

Grieshop, A. P., Logue, J. M., Donahue, N. M., and Robinson, A. L.: Laboratory investigation of photochemical oxidation of organic aerosol from wood fires - Part 1: Measurement and simulation of organic aerosol evolution, Atmos. Chem. Phys. Discuss., 8, 15 699–15 737, 2008, http://www.atmos-chem-phys-discuss.net/8/15699/2008/.

Herndon, S. C., Onasch, T. B., Wood, E. C., Kroll, J. H., Canagaratna, M. R., Jayne, J. T., Zavala, M. A., Knighton, W. B., Mazzoleni, C., Dubey, M. K., Ulbrich, I. M., Jimenez, J. L., Seila, R., Gouw, J. A. d., Foy, B. d., Fast, J., Molina, L. T., Kolb, C. E., and Worsnop, D. R.: The correlation of secondary organic aerosol with odd oxygen in a megacity outflow, Geophys. Res. Lett., 35, L15804, doi:10.1029/2008GL034058, 2008.

Hoffer, A., Gelencsér, A., Blazsó, M., Guyon, P., Artaxo, P., and Andreae, M. O.: Diel and seasonal variations in the chemical composition of biomass burning aerosol, Atmos. Chem. Phys., 6, 3505–3515, 2006

Huffman, J. A., Ziemann, P. J., Jayne, J. T., Worsnop, D. R., and Jimenez, J. L.: Development and characterization of a fast-stepping/scanning thermodenuder for chemically-resolved aerosol volatility measurements, Aerosol Sci. Tech., 42(5), 395–407, 2008.

Jimenez, J. L., Jayne, J. T., Shi, Q., Kolb, C. E., Worsnop, D. R., Yourshaw, I., Seinfeld, J. H., Flagan, R. C., Zhang, X. F., Smith, K. A., Morris, J. W., and Davidovits, P.: Ambient aerosol sampling using the Aerodyne Aerosol Mass Spectrometer, J. Geophys. Res.-Atmos., 108(D7), 8425, doi:10.1029/2001JD001213, 2003.

Koppmann, R., von Czapiewski, K., and Reid, J. S.: A review of biomass burning emissions, part I: gaseous emissions of carbon monoxide, methane, volatile organic compounds, and nitrogen containing compounds, Atmos. Chem. Phys. Discuss., 5, 10 455–10 516, 2005, http://www.atmos-chem-phys-discuss.net/5/10455/2005/.

Laboratory studies of the atmospheric aging of wood smoke – Part 2

A. P. Grieshop et al.

Title Page

Abstract | Introduction

Conclusions | References

Tables | Figures

|◄ | ►|

◄ | ►

Back | Close

Full Screen / Esc

Printer-friendly Version

Interactive Discussion

Lanz, V. A., Alfarra, M. R., Baltensperger, U., Buchmann, B., Hueglin, C., and Prévôt, A. S. H.: Source apportionment of submicron organic aerosols at an urban site by factor analytical modelling of aerosol mass spectra, Atmos. Chem. Phys., 7, 1503–1522, 2007, http://www.atmos-chem-phys.net/7/1503/2007/.

Lee, S., Kim, H. K., Yan, B., Cobb, C. E., Hennigan, C., Nichols, S., Chamber, M., Edgerton, E. S., Jansen, J. J., Hu, Y. T., Zheng, M., Weber, R. J., and Russell, A. G.: Diagnosis of aged prescribed burning plumes impacting an urban area, Environ. Sci. Technol., 42(5), 1438–1444, 2008.

Lipsky, E. M. and Robinson, A. L.: Effects of dilution on fine particle mass and partitioning of semivolatile organics in diesel exhaust and wood smoke, Environ. Sci. Technol., 40(1), 155–162, 2006.

Nopmongcol, U., Khamwichit, W., Fraser, M. P., and Allen, D. T.: Estimates of heterogeneous formation of secondary organic aerosol during a wood smoke episode in Houston, Texas, Atmos. Environ., 41(14), 3057–3070, 2007.

Reid, J., Hobbs, P., Ferek, R., Blake, D., Martins, J., Dunlap, M., and Liousse, C.: Physical, chemical, and optical properties of regional hazes dominated by smoke in Brazil, J. Geophys. Res., 103(D24), 32 059–32 080, 1998.

Reid, J. S., Koppmann, R., Eck, T. F., and Eleuterio, D. P.: A review of biomass burning emissions part II: intensive physical properties of biomass burning particles, Atmos. Chem. Phys., 5, 799–825, 2005, http://www.atmos-chem-phys.net/5/799/2005/.

Robinson, A. L., Donahue, N. M., Shrivastava, M. K., Weitkamp, E. A., Sage, A. M., Grieshop, A. P., Lane, T. E., Pierce, J. R., Pandis, S. N.: Rethinking Organic Aerosols: semivolatile Emissions and Photochemical Aging, Science, 315, 1259–1262, 2007.

Sage, A. M., Weitkamp, E. A., Robinson, A. L., and Donahue, N. M.: Evolving mass spectra of the oxidized component of organic aerosol: results from aerosol mass spectrometer analyses of aged diesel emissions, Atmos. Chem. Phys., 8, 1139–1152, 2008, http://www.atmos-chem-phys.net/8/1139/2008/.

Schauer, J. J., Kleeman, M. J., Cass, G. R., and Simoneit, B. R. T.: Measurement of emissions from air pollution sources. 2. C-1 through C-30 organic compounds from medium duty diesel trucks, Environ. Sci. Technol., 33(10), 1578–1587, 1999.

Schauer, J. J., Kleeman, M. J., Cass, G. R., and Simoneit, B. R. T.: Measurement of emissions from air pollution sources. 3. C-1-C-29 organic compounds from fireplace combustion of

Laboratory studies of the atmospheric aging of wood smoke – Part 2

A. P. Grieshop et al.

wood, Environ. Sci. Technol., 35(9), 1716–1728, 2001.

Schneider, J., Weimer, S., Drewnick, F., Borrmann, S., Helas, G., Gwaze, P., Schmid, O., Andreae, M. O., and Kirchner, U.: Mass spectrometric analysis and aerodynamic properties of various types of combustion-related aerosol particles, Int. J. Mass Spectrom., 258(1–3), 37–49, 2006.

Shrivastava, M. K., Lipsky, E. M., Stanier, C. O., and Robinson, A. L.:, Modeling semivolatile organic aerosol mass emissions from combustion systems, Environ. Sci. Technol., 40(8), 2671–2677, 2006.

Simoneit, B. R. T., Schauer, J. J., Nolte, C. G., Oros, D. R., Elias, V. O., Fraser, M. P., Rogge, W. F., and Cass, G. R.: Levoglucosan, a tracer for cellulose in biomass burning and atmospheric particles, Atmos. Environ., 33(2), 173–182, 1999.

Takegawa, N., T. Miyakawa, K. Kawamura, and Kondo, Y.: Contribution of selected dicarboxylic and omega-oxocarboxylic acids in ambient aerosol to the m/z 44 signal of an aerodyne aerosol mass spectrometer, Aerosol Sci Tech., 41(4), 418–437, 2007.

Ulbrich, I. M., Canagaratna, M. R., Zhang, Q., Worsnop, D. R., and Jimenez, J. L.: Interpretation of organic components from positive matrix factorization of aerosol mass spectrometric data, Atmos. Chem. Phys. Discuss., 8, 6729–6791, 2008,
http://www.atmos-chem-phys-discuss.net/8/6729/2008/.

Ulbrich, I. M. and Jimenez, J. L.: AMS Spectral Database, available at: http://cires.colorado.edu/jimenez-group/AMSsd/, June 2008, 2008.

Volkamer, R., Jimenez, J. L., San Martini, F., Dzepina, K., Zhang, Q., Salcedo, D., Molina, L. T., Worsnop, D. R., and Molina, M. J.: Secondary organic aerosol formation from anthropogenic air pollution: Rapid and higher than expected., Geophys. Res. Lett., 33, L17811, doi:10.1029/2006GL026899, 2006.

Wehner, B., Philippin, S., and Wiedensohler, A.: Design and calibration of a thermodenuder with an improved heating unit to measure the size-dependent volatile fraction of aerosol particles, J. Aerosol Sci., 33(7), 1087–1093, 2002.

Weitkamp, E. A., Sage, A. M., Pierce, J. R., Donahue, N. M., and Robinson, A. L.: Organic aerosol formation from photochemical oxidation of diesel exhaust in a smog chamber, Environ. Sci. Technol., 41(20), 6969–6975, 2007.

Zhang, J. Y., Huff Hartz, K. E., Pandis, S. N., and Donahue, N. M.: Secondary organic aerosol formation from limonene ozonolysis: homogeneous and heterogeneous influences as a function of NO_x, J. Phys. Chem. A, 110(38), 11 053–11 063, 2006.

Laboratory studies of the atmospheric aging of wood smoke – Part 2

A. P. Grieshop et al.

Title Page

Abstract	Introduction
Conclusions	References
Tables	Figures

|◄ | ►|

◄ | ►

Back | Close

Full Screen / Esc

Printer-friendly Version

Interactive Discussion

Zhang, Q., Alfarra, M. R., Worsnop, D. R., Allan, J. D., Coe, H., Canagaratna, M. R., and Jimenez, J. L.: Deconvolution and quantification of hydrocarbon-like and oxygenated organic aerosols based on aerosol mass spectrometry, Environ. Sci. Technol., 39(13), 4938–4952, 2005a.

5 Zhang, Q., Worsnop, D. R., Canagaratna, M. R., and Jimenez, J. L.: Hydrocarbon-like and oxygenated organic aerosols in Pittsburgh: insights into sources and processes of organic aerosols, Atmos. Chem. Phys., 5, 3289–3311, 2005b, http://www.atmos-chem-phys.net/5/3289/2005/.

Zhang, Q., Jimenez, J. L., Canagaratna, M. R., Allan, J. D., Coe, H., Ulbrich, I., Alfarra, M.
10 R., Takami, A., Middlebrook, A. M., Sun, Y. L., Dzepina, K., Dunlea, E., Docherty, K., De-Carlo, P. F., Salcedo, D., Onasch, T., Jayne, J. T., Miyoshi, T., Shimono, A., Hatakeyama, S., Takegawa, N., Kondo, Y., Schneider, J., Drewnick, F., Weimer, S., Demerjian, K., Williams, P., Bower, K., Bahreini, R., Cotrell, L., Griffin, R. J., Rautiainen, J., Sun, J. Y., Zhang, Y. M., and Worsnop, D. R.: Ubiquity and dominance of oxygenated species in organic aerosols in
15 anthropogenically-influenced Northern Hemisphere mid-latitudes, Geophys. Res. Lett., 34, L13801, doi:10.1029/2007GL029979, 2007.

Laboratory studies of the atmospheric aging of wood smoke – Part 2
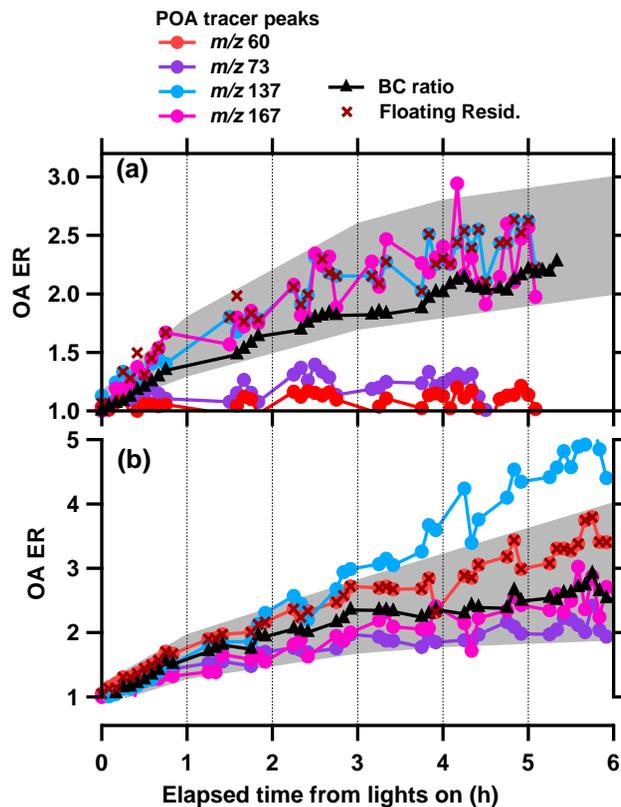
A. P. Grieshop et al.

Fig. 1. OA enhancement ratios estimated using BC and residual decomposition methods. The data are from experiments 3 **(a)** and 5 **(b)** described in Tables 1 and 2 in the companion manuscript (Grieshop et al., 2008).
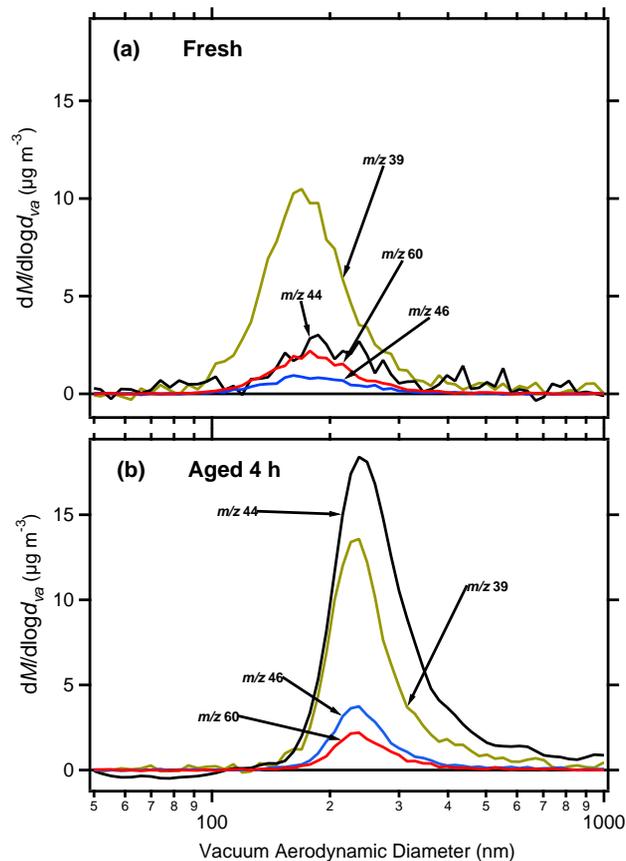
Fig. 2. Size distribution of selected AMS fragments of **(a)** fresh and **(b)** aged wood smoke from a flaming Yellow Pine experiment. Data are from Experiment 4 summarized in Tables 1 and 2 of the companion manuscript (Grieshop et al., 2008).
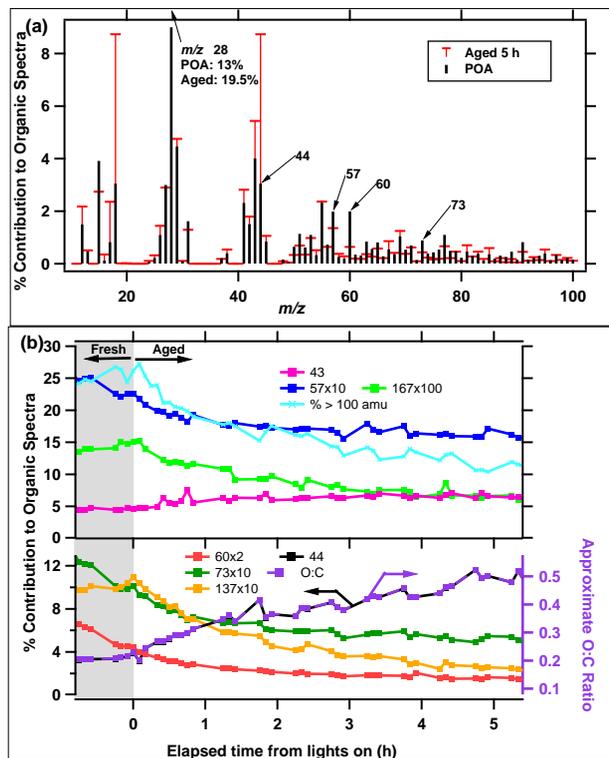
Fig. 3. (a) Mass spectra of fresh and aged wood smoke OA. **(b)** Time series of key AMS mass fragments: m/z 60, 73, 137 and 167 are indicators of primary or fresh wood smoke emissions, and m/z 44 and 43 are indicators of oxidation and aging. Fractional contributions are shown relative to the OA mass neglecting the contribution from m/z 28 to facilitate comparison with published AMS data. Including the additional mass at m/z 28 would decrease these values by 15–25%. The signals for m/z 57, 60, 73, 137 and 167 have been scaled by the factors listed in the legend of (b). Data are from Experiment 5 (smoldering experiment with Yellow Pine) listed in Tables 1 and 2 of the companion manuscript (Grieshop et al., 2008).

Full Screen / Esc

Printer-friendly Version

Interactive Discussion
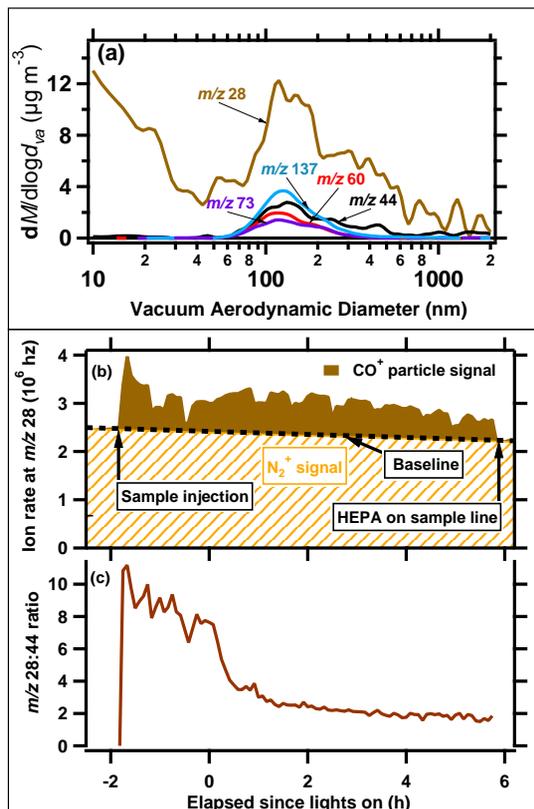
Fig. 4. Evidence for the substantial contribution of OA to the AMS signal at m/z 28. **(a)** Size distributions of key mass fragments. Time series of **(b)** m/z 28 ion rate and **(c)** ratio of estimated particle contribution at m/z 28 to m/z 44. The hatched area in (b) indicates the AMS signal apportioned to gas-phase N_2^+; the filled area indicates the signal apportioned to particle-phase OA (CO^+). Data are from a high-mass concentration flaming Yellow Pine experiment (Experiment 4) (Grieshop et al., 2008).
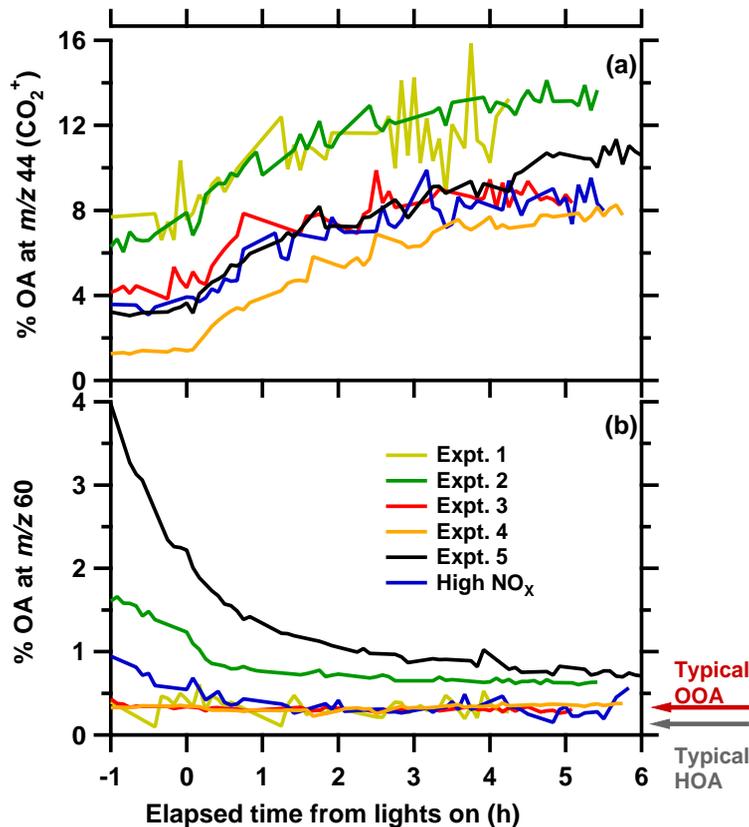
Fig. 5. Time series of fractional contributions from **(a)** m/z 44 and **(b)** 60 to total organic aerosol mass measured in each experiment. Fractional contributions are shown relative to the OA mass neglecting the contribution from m/z 28 to facilitate comparison with published AMS data. Arrows in (b) show typical contribution at m/z 60 in typical OOA and HOA spectra (see e.g. Zhang et al., 2005a). See the companion manuscript (Grieshop et al., 2008) for experimental details.
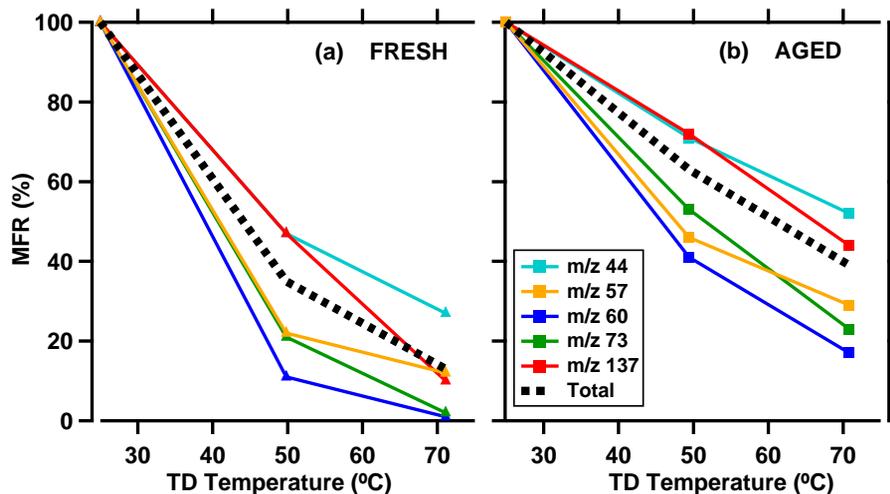
Fig. 6. Average thermograms of thermodenuder MFR data for **(a)** fresh and **(b)** aged wood smoke OA. The dash lines indicate average of MFR of the entire OA. The colored symbols indicate data for selected AMS mass fragments. The colored lines are intended to guide the eye.
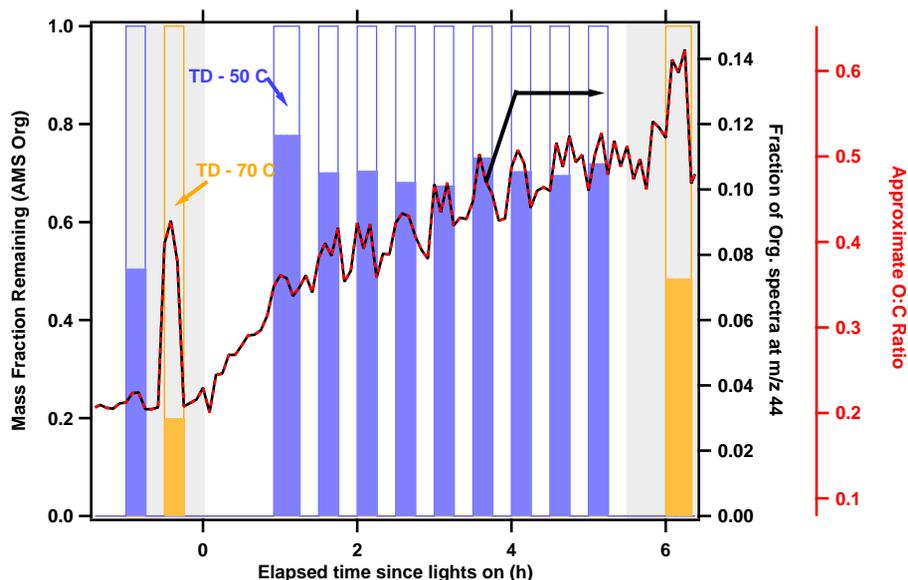
Fig. 7. Time series of measured MFR at 50 and 70°C (left axis) and fractional contribution at m/z 44 (right axis). Bars show periods when sample was drawn through the thermodenuder and the filled areas show the OA MFR. Also shown is an estimate of OA atomic O:C ratio based on the relation from Aiken et al. (2008). Fractional contribution at m/z 44 shown relative to the OA mass neglecting the contribution from m/z 28 to facilitate comparison with other AMS data.
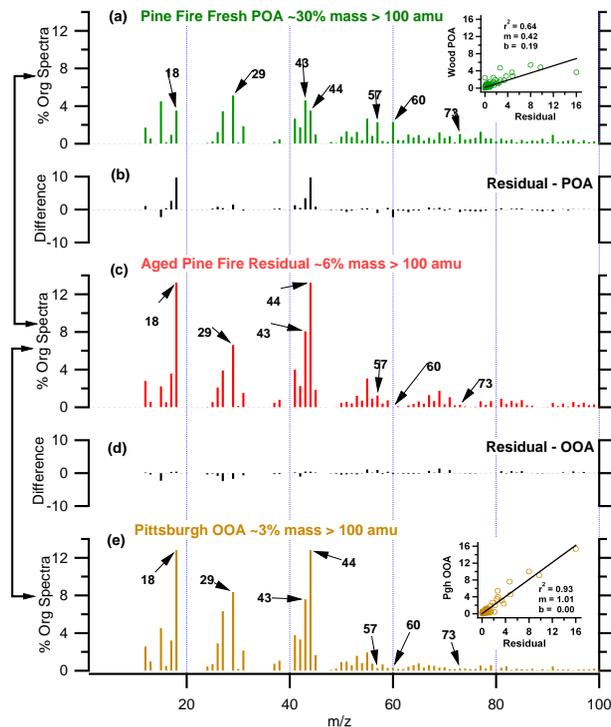
Fig. 8. Comparison of AMS spectra **(a)** fresh wood smoke OA, **(c)** residual of aged wood smoke OA; and **(e)** the OOA factor extracted from Pittsburgh ambient measurements (Zhang et al., 2005a). The spectra shown in panels **(b)** and **(d)** are difference between the residual and other spectra. Contributions at m/z 28 in the laboratory spectra have been zeroed and the spectra renormalized to allow direct comparison with Pittsburgh OOA. The inset scatter plots show linear regressions of the wood-smoke residual with wood-POA (a) and Pittsburgh OOA (e) with contributions at m/z 16, 17, 18 and 28 removed. Data are from experiment 5 listed in Tables 1 and 2 of the companion manuscript (Grieshop et al., 2008).
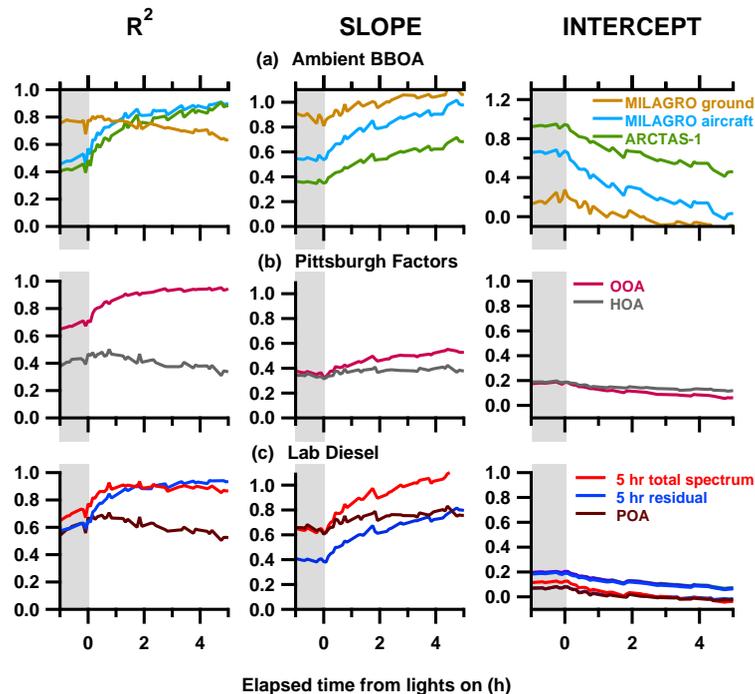
Fig. 9. Comparison of laboratory AMS OA mass spectra with reference spectra from other laboratory and field studies. Each row shows time series of R^2, slope and intercept values of linear regressions of the time-evolving wood-smoke spectra with a set of fixed reference spectra. **(a)** The first row shows comparisons with BBOA spectra measured in or derived from ambient studies. **(b)** The second row shows comparisons with ambient HOA and OOA spectra measured in Pittsburgh. **(c)** The third row shows comparisons with spectra from diesel aging experiments (Sage et al., 2008). BBOA spectra provided by J. L. Jimenez. Chamber data are from Experiment 5 listed in Tables 1 and 2 of the companion manuscript (Grieshop et al., 2008).